water

MDPI

Article

Estimation of Precipitation Fraction in the Soil Water of the Hillslope Vineyard Using Stable Isotopes of Water

Zoran Kovač [1,*], Vedran Krevh [2], Lana Filipović [2], Jasmina Defterdarović [2], Borna-Ivan Balaž [1] and Vilim Filipović [2,3]

[1] Department of Geology and Geological Engineering, Faculty of Mining, Geology and Petroleum Engineering, University of Zagreb, 10000 Zagreb, Croatia
[2] Department of Soil Amelioration, Faculty of Agriculture, University of Zagreb, 10000 Zagreb, Croatia
[3] Future Regions Research Centre, Geotechnical and Hydrogeological Engineering Research Group, Federation University, Gippsland, VIC 3841, Australia
* Correspondence: zoran.kovac@rgn.unizg.hr

Abstract: This paper presents research related to the estimation of the precipitation fraction in the soil water of a sloped vineyard at the SUPREHILL Critical Zone Observatory (CZO) in Zagreb, Croatia. Numerous investigations have shown that exploration of hillslope soils can be very challenging due to the existence of heterogeneity and different soil properties, as well as due to anthropogenically induced processes, which can affect precipitation infiltration and soil water flow. Within this research, physicochemical soil properties, soil water content (SWC), and isotopic composition of soil water and precipitation (δ^2H and $\delta^{18}O$) have been examined. The isotopic signature of soil water was monitored in 24 points, at 4 depths, throughout the hillslope vineyard. Soil water isotopic composition from all monitoring points coincided with the Local Meteoric Water Line (LMWL), with almost no variability at 100 cm depth, which was consistent with the smallest variation of SWC at 80 cm depth and indicated that most of water mixing takes place in the shallower part of the hillslope. Results suggested the existence of heterogeneity, uneven erosion processes in the footslope of the observed vineyard, and different infiltration patterns. Fractions of precipitation varied significantly depending on the depth and position in the vineyard, from approximately 1% up to 98%, where more precipitation fraction has been determined in the surface and subsurface runoff. Additionally, statistical analysis and a more detailed evaluation of precipitation fractions at the 40 cm depth, where wick lysimeters are installed, have shown that C_{org} content is related to the silt fraction, while the first results indicate that the infiltration patterns were dependent on the common influence of all observed physicochemical properties.

Keywords: sloped vineyard; soil water; infiltration; precipitation fraction; stable isotopes of oxygen and hydrogen; soil properties; mass balance mixing model

Citation: Kovač, Z.; Krevh, V.; Filipović, L.; Defterdarović, J.; Balaž, B.-I.; Filipović, V. Estimation of Precipitation Fraction in the Soil Water of the Hillslope Vineyard Using Stable Isotopes of Water. *Water* **2023**, *15*, 988. https://doi.org/10.3390/w15050988

Academic Editor: Paul Kucera

Received: 9 February 2023
Revised: 27 February 2023
Accepted: 2 March 2023
Published: 4 March 2023

1. Introduction

Investigation of hillslope soils can be very challenging. Numerous hydrological studies of soils in the last years have been focused on problems related to the determination of different types of flows in soil, as well as to human practices, processes, slope, and soil characteristics that affect soil water movement [1–8]. In general, infiltration of precipitation presents a complex process that can be described as preferential or piston flow. Preferential flow water is channeled through more permeable pathways, while with piston flow, water from recent precipitation forces the older soil water to flow downward [9].

It has been shown that soil porosity, soil water content, soil structure, soil texture, soil compaction, and vegetation can affect infiltration of surface water [9,10], but also that soil hydrophobicity can reduce water infiltration into the soil [11]. Organic matter can also be important because some research showed that soil organic carbon, which corresponds to

the high levels of organic matter, can enhance permeability and water availability, as well as hydraulic conductivity of soil by improving aggregate stability and porosity [12–15]. Previous results also showed that subsurface hillslope flow is different in wet and dry conditions. In wet conditions, subsurface lateral flow prevails, while in dry conditions, flow is dominantly vertical [16–18]. Furthermore, it has been shown that soil erosion can play a crucial role in hillslope hydrology, causing soil heterogeneity [5], where the footslope can have a deeper loose layer compared to the hilltop [8]. The soil heterogeneity can also cause preferential flow on the whole hillslope, local preferential flow, or surface runoff [2]. Additionally, to determine water flow and solute transport, chemical tracer experiments [19,20] as well as dye tracers have been used [3,21].

Stable isotopes of oxygen and hydrogen in soil water have been used in numerous studies of soil and unsaturated zone [22–26], while some of them were related to the hillslopes [27,28]. In general, there are two types of water that should be distinguished: mobile and bulk water. Mobile water should follow the one of the precipitation but can have high variability of water isotopic composition in a defined soil depth over space and time [29,30]. However, some research showed that macropore flow can have a different isotopic signature with respect to the precipitation [31] and can possibly indicate mixing between water from the soil matrix and the macropore flow [32]. It has been shown that the kinetic fractionation usually cannot be seen in mobile water, but can be seen in bulk soil water, and is globally limited to the upper 30 cm of the soil in most soil water isotope hydrology studies [32,33]. It must be emphasized that local precipitation can have strong temporal variation in isotope composition due to temperature and different isotope effects [34], which can consequently result in isotopic heterogeneities [35,36] where small pores may contain water similar to older precipitation, while larger pores could consist of more recent precipitation [37,38]. The newest research has shown that the isotopic composition of soil bulk water should be different from evaporating water, although the difference can be too small to affect the evaporative water loss calculation [39]. Furthermore, it has been shown that soil tension, water–mineral interaction, and soil particle surface adsorption can have an influence on the soil water isotopic signature and its variations [40–44].

In the last few years, much research has been conducted in the wider Zagreb area. Most of the research was focused on the identification of the relationship between Zagreb aquifer and Sava River using statistical [45,46] and isotope techniques [47–49]. Soil and unsaturated zone research were focused to the estimation of water flow and the transport of potentially toxic metals [50], and the evaluation of physical and chemical properties on soil permeability [51]. Newest soil research is related to the sorption of cadmium, zinc, and cooper in the dominant soils of the Zagreb aquifer [52], the definition of nickel and chromium origin in Fluvisols [53], as well as to the estimation of precipitation infiltration through the unsaturated zone into the Zagreb aquifer using cross-correlation analysis and stable isotopes of water [54]. Regarding investigated hillslope vineyard, the first initial isotopic insight suggested that preferential flow can be expected to a maximum depth of 80 cm [55], while it has been also found that erosion-affected soil structural properties can influence soil hydraulic properties and soil water dynamics [8].

The objectives of this study were to: (1) investigate soil water isotopic signature in 24 monitoring points at 4 different depths in the hillslope vineyard, (2) estimate the precipitation fraction in soil water using the isotope mass balance mixing model, and (3) determine soil properties that influence water infiltration.

2. Materials and Methods

The research area (SUPREHILL Critical Zone Observatory (CZO); https://sites.google.com/view/suprehill/) ((accessed on 11 November 2022) is located in the agricultural sloped area within the experimental field Jazbina in Zagreb, Croatia (Figure 1). It is a vineyard with rows separated by grassed inter-row areas (2 m wide). The soil type is classified according to World Reference Base (WRB) classification system as Dystric Luvic Stagnosol [8]. The hillslope is separated into three segments: hilltop, backslope, and

footslope. The sloping between the segments was determined using an unmanned aerial vehicle (UAV) and Agisoft Metashape software (Agisoft LLC., St. Petersburg, Russia, ver. 1.7.5), with the sloping between the hilltop and backslope being 17.5%, and the sloping between backslope and footslope was 25.4%. Additional to the vineyard-row-oriented south-east sloping, perpendicular-to-row sloping is present, with 7.3% at the hilltop and backslope and 4.4% at the footslope.

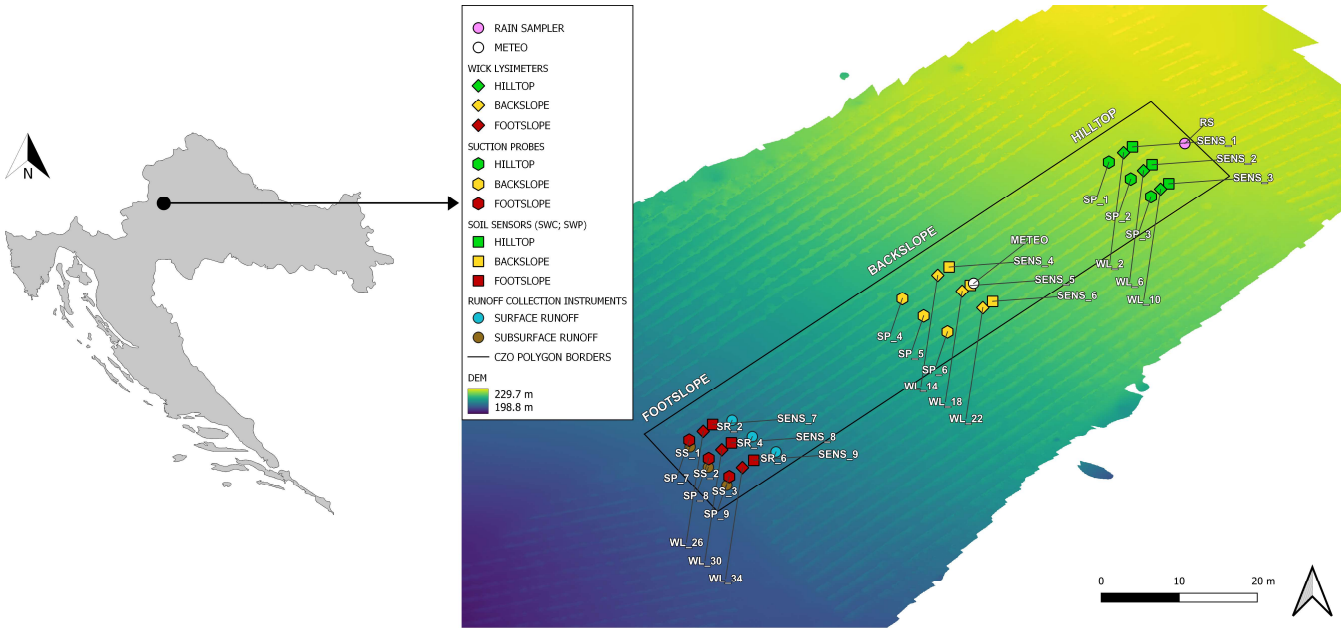

Figure 1. Scheme of the installed research setup at the SUPREHILL Critical Zone Observatory (CZO) (hillslope vineyard), presented on a digital elevation model (DEM).

In Figure 1 locations of all the used monitoring points can be seen. Within this research, four different types of instruments have been installed for sampling soil water. At the surface level, for capturing surface water runoff, self-constructed instruments were installed at the footslope (2 × 2 m) in 3 repetitions (vineyard rows). At the 40 cm depth, for the measurement of near surface drainage, passive wick lysimeters were used. They were installed at the hillslope, backslope, and footslope, between two vines, in three repetitions. They have dimensions of 250 × 250 × 40 mm. Their surface is covered with a filter mesh (1 × 1 mm) to prevent clogging, while fiberglass is placed inside the lysimeter. At 60 cm depth, a self-constructed instrument for collecting subsurface runoff was installed, also in 3 repetitions in rows at the footslope. For sampling water from 100 cm depth, suction probes (UGT Umwelt-Geräte-Technik, Müncheberg, Germany) with a ceramic cup were installed at the hillslope, backslope, and footslope, also in 3 repetitions (vineyard rows). To summarize, soil water was sampled from depths of 20 cm, 40 cm, 60 cm, and 100 cm. From 20 cm (SR_2, SR_4 and SR_6) and 60 cm (SS_1, SS_2 and SS_3) depth water was sampled only at the footslope, while from 40 cm (WL_2, WL_6, WL_10, WL_14, WL_18, WL_22, WL_26, WL_30, WL_34) and 100 cm (SP_1 to SP_9) depth water was sampled additionally at the hillslope and backslope. In this research, the closest monitoring points in rows were used for data evaluation, resulting in a total of 24 monitoring points of soil water plus rain sampler (RS). For the construction of the Local Meteoric Water Line (LMWL) and further analysis, all data related to the precipitation isotopic signature have been used except for August 2022, due to technical issues with rain sampler and significant evaporation of the sample which resulted in negative d-excess and significant shift from the LMWL.

Data used in this research can be generally divided into four groups: meteorological data, soil water content (SWC), soil physicochemical parameters, and stable isotopes of oxygen and hydrogen in precipitation and soil water. All data are related to the period from

February 2021 to September 2022. Meteorological and SWC data are presented as daily data, and stable isotopes are presented as monthly data, while physicochemical parameters were defined at the establishment of the SUPREHILL CZO. All data was processed, and basic statistical parameters (average, median, maximum, minimum, standard deviation-SD, and coefficient of variation–CV) were calculated with Microsoft Excel, while Tibco Statistica (version 14.0.0.15) was used for the construction of boxplots and correlation analysis.

Within this paper, the sum of daily precipitation and evapotranspiration data is presented, as well as daily average air temperature. Daily reference evapotranspiration was calculated via the Penman–Monteith equation [56], while all meteorological parameters were gathered using a meteorological station (ATMOS41, METER Group, Inc., Pullman, WA, USA) installed in the backslope position of the hillslope at a 2 m height.

SWC was measured at the hourly intervals with capacitance sensors (TEROS 10/TEROS 12, METER Group, Inc., Pullman, WA, USA). Sensors were installed in vineyard rows, in between 2 vines, in 3 repetitions (3 different vineyard rows) at 20, 40, 60, and 80 cm depth, to capture the soil water dynamics near the installed soil water sampling instruments. Sensors at 40 and 80 cm depth were installed at the hillslope, backslope, and footslope, near the wick lysimeters and suction probes, while at 20 and 60 cm, they were installed at the footslope near the surface and subsurface runoff instruments.

Sampling of disturbed soil samples was performed at 3 depths (0–30, 30–60, and 60–90 cm) at the hillslope, backslope, and footslope, in 3 repetitions. Granulometric soil composition analysis was performed according to [57], while organic carbon content (C_{org}) was determined using sulfochromic oxidation according to [58]. Values of the bulk density have been estimated using HYPROP-FIT for the hilltop, backslope, and footslope for 4 depths (0–20, 20–40, 40–60, and 60–90 cm) and 3 vineyard rows [59], while, for this research, only the average values for depth up to 40 cm have been used. According to the United States Department of Agriculture soil classification system (USDA) [60], soils have been classified as silt loam or silty clay loam for all three depths [55].

Stable isotopes of oxygen and hydrogen ($\delta^{18}O$ and $\delta^{2}H$) in precipitation and soil water were determined at the Laboratory for Spectroscopy of the Faculty of Mining, Geology and Petroleum Engineering, University of Zagreb, using laser absorption spectroscopy (Liquid Water Isotope Analyzer LWIA-45-EP, Los Gatos Research, San Jose, USA). It has been shown that analyzers which use laser spectroscopy are fully suitable for the high precision isotopic analysis of natural waters [61]. Data were analyzed using Laboratory Information Management System (LIMS for lasers 2015) [62]. The results are reported as δ values per mill (‰) relative to the standard [63–65]:

$$\delta = \frac{R_{sample}}{R_{standard}} - 1 \quad (1)$$

where R_{sample} and $R_{standard}$ stand for the isotope ratio in the sample ($R = {}^{2}H/{}^{1}H$ and $R = {}^{18}O/{}^{16}O$) and standard material, respectively. This means that δ value expresses the relative difference in ‰ of the isotope ratio R in the sample to the defined (known) isotope ratio in the international reference material (standard). Within this research, all results are presented with respect to VSMOW (Vienna Standard Mean Ocean Water), with measurement precision of ± 0.19‰ for $\delta^{18}O$ and ± 0.9‰ for $\delta^{2}H$. Deuterium excess (d-excess) has been defined according to Dansgaard [66] with a global mean slope of 8. For the $\delta^{18}O$ and $\delta^{2}H$ analysis of cumulative monthly precipitation samples, a rain collector RS-1 (Palmex Ltd., Zagreb, Croatia), whose design allows evaporation-free rain sampling [67] and is suitable for most hydrology investigations [68], was installed at the top of the hillslope at 1 m above ground.

In this research, the isotopic signature of soil water has been evaluated in 24 monitoring points. Soil water from the deepest observed soil depth (100 cm) was approximated as non-mobile water due to small variability of the isotopic composition (presented in the results and discussion section), which is probably related to the bulk water and/or older precipitation, i.e., precipitation that fell before the investigated time period. Small variability of the isotopic composition also suggests that most of the water mixing in the hillslope

vineyard is occurring in the first 100 cm depth (Figure 2). The isotopic signature of recent precipitation (the one that fell within the investigated time period) was taken as the only input of recharge, while precipitation infiltration was estimated through calculation of precipitation fractions at 20 cm, 40 cm, and 60 cm depth using the two-end member mass balance equation, where the sum of the end member contributions is usually expressed as fractions (f) equal to 1 [47,69–71]. In general, infiltration presents the process by which water that falls on the surface enters the soil. However, it must be emphasized that the fraction of recent precipitation in the observed monitoring point presents the part of the water which has infiltrated into the soil, but which has been captured by the instrument. From that perspective, it presents infiltrated water, but probably does not present the total amount of the infiltrated water. Precipitation fractions were estimated by two-component mixing model using following equations:

$$f_{snmw} + f_p = 1 \quad (2)$$

$$f_{snmw} \times \delta^{18}O_{snmw} + f_p \times \delta^{18}O_p = \delta^{18}O_{smw} \quad (3)$$

where f_{snmw} and f_p are the soil non-mobile water and precipitation fractions (end members, Figure 2), $\delta^{18}O_{smw}$ is the isotopic composition of oxygen in the soil water of the investigated monitoring point (isotopic composition is the consequence of mixing between end members), while $\delta^{18}O_{snmw}$ and $\delta^{18}O_p$ are the isotopic compositions of oxygen in the soil non-mobile water and precipitation, respectively.

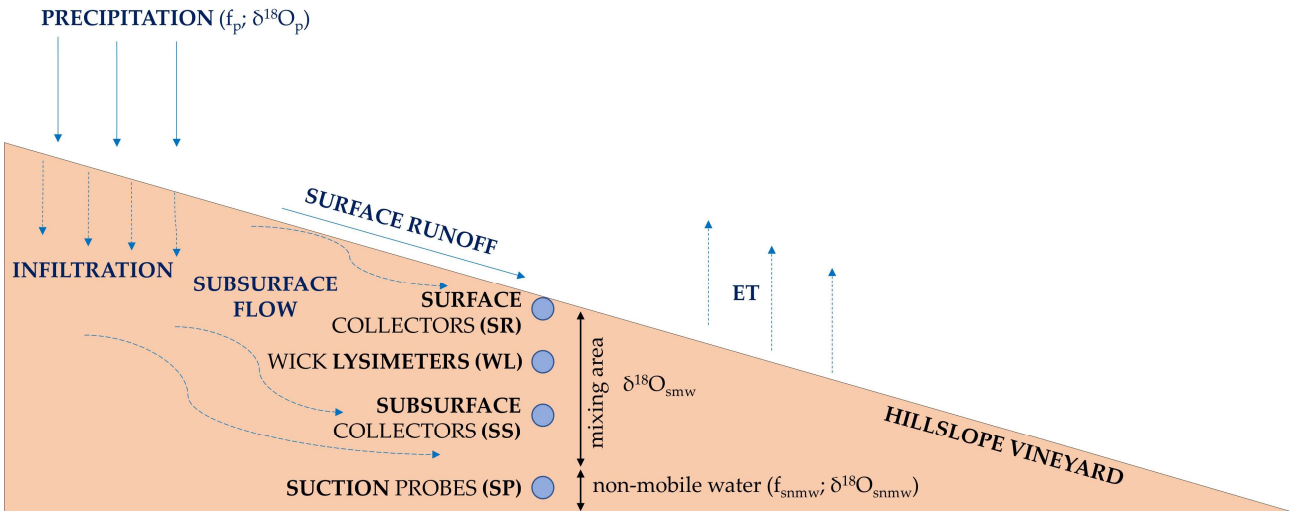

Figure 2. Scheme of water mixing in the hillslope vineyard.

3. Results and Discussion

3.1. Evaluation of Meteorological Parameters

Variations of precipitation, evapotranspiration, and air temperature are shown in Figure 3. In the observed period, 247 days had precipitation. Daily precipitation varied from 0.017 mm to 54.98 mm, with average of 5.27 mm. Average daily temperature was 13.91 °C and ranged from −5.14 °C to 29.9 °C. According to the values of average yearly air temperature, which can be seen in the Croatian Meteorological and Hydrological Service [72], year 2021 in the study area has been defined as a warm year, while year 2022 has been defined as an extremely warm year. On the other hand, yearly sums of precipitation suggest normal, expected values in both 2021 and 2022. Daily reference evapotranspiration reached up to 6.30 mm, with an average of 2.49 mm per day. The total daily reference evapotranspiration during the observed period was 1510.4 mm, higher than the total precipitation of 1301.79 mm. In the most monitoring points, soil water was only captured in the autumn to spring period due to the existence of warm and extremely

warm summer periods. This is consistent with the measured volumes presented in Figure 4. In general, within the summer months, isotopic composition of soil water was measured only for surface runoff. In total, without considering samples related to the precipitation, for 228 samples the isotopic composition has been defined. Due to the lack of data, the mass balance model has been applied using average values calculated based on months where at least half of the monitoring points had measured isotopic signature, resulting in the usage of 191 of 228 samples. Volume from suction cups is not presented due to challenging sampling of soil water in the deepest observed layer, i.e., very small amounts were available.

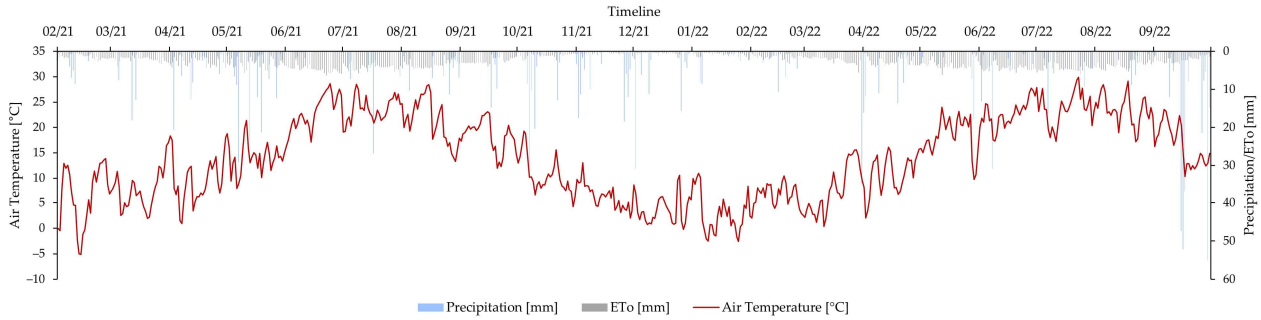

Figure 3. Variation of meteorological parameters in the observed period.

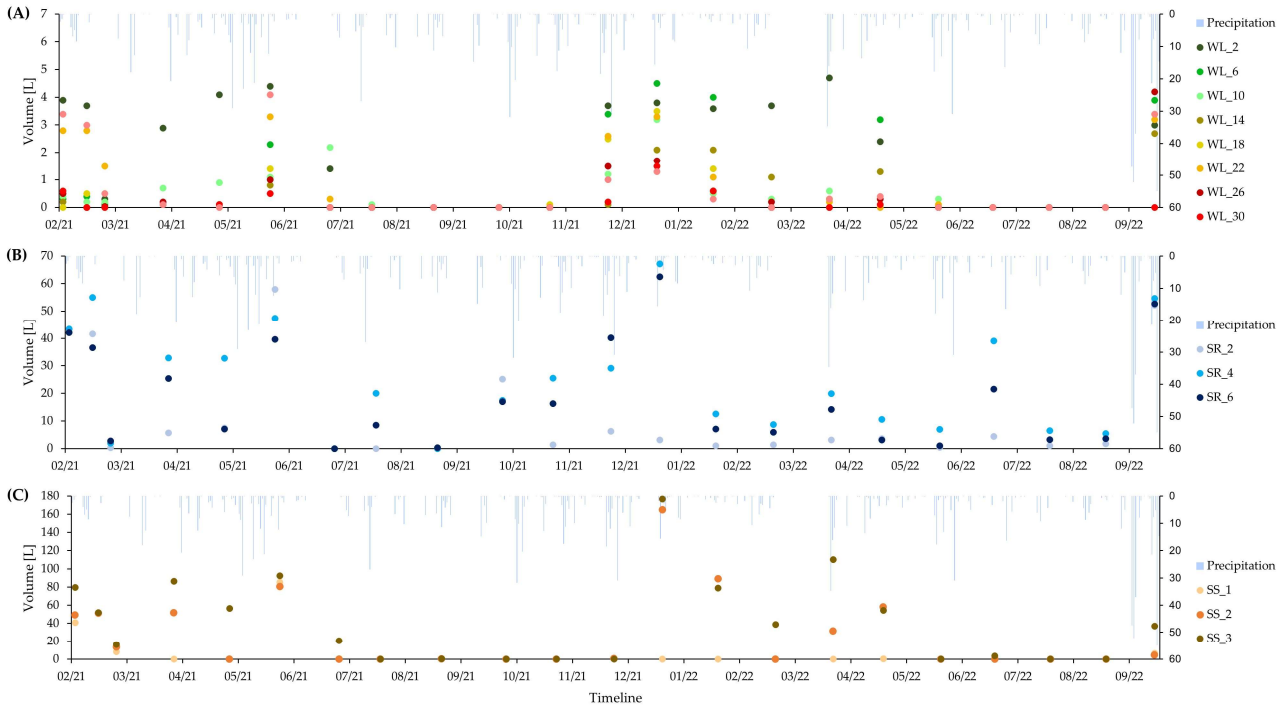

Figure 4. Water volume measured in different sampling instruments in the observed period: (**A**) wick lysimeters; (**B**) surface runoff; (**C**) subsurface runoff.

3.2. Variability of Soil Water Content and Granulometric Composition

Variation of the SWC is presented in Figure 5, while basic statistical parameters for all monitoring points are shown in Table 1. It can be clearly seen that probes in all locations and depths showed similar reaction in the summer months, i.e., SWC drastically dropped. Additionally, it can be seen that variation of SWC was not identical if the location on the hillslope and depth of the sensor are taken into account. For example, SR_2 (SENS_7) had the lowest average (0.26 cm^3 cm^{-3}) SWC, but one of the biggest CV (0.25). Some sensors above suction probes (SP_3 and SP_8) had high (0.24 and 0.21, respectively) CV values,

while some (SP_9) had one of the highest average (0.34) SWC and one of the lowest CV (0.12). However, when evaluating average values of all sensors at the same depths, the results suggested that surface runoff corresponded to the lowest average and median value, as well as the lowest minimum value. Subsurface runoff had similar average and median values, but a lower standard deviation and CV value, when comparing them to the sensors at 40 cm depth. The deepest sensors had the highest minimum values as well as the lowest standard deviation and a much lower CV. This suggested that variation of the SWC in 100 cm depth, where suction probes were installed, was even lower. Additionally, this corresponds to the results of the previous research, where results suggested that most of the preferential flow can be expected at up to 80 cm depth [55]. As shown in the Figure 1, different slopes have been observed in the investigated hillslope vineyard. The slope between the hilltop and backslope is 17.5%, while between backslope and footslope it is 25.4%. In addition to the vineyard-row, which has south-east sloping, perpendicular-to-row sloping has been also observed, with 7.3% at the hilltop and backslope, and 4.4% at the footslope. When observing all locations in the vineyard, using data from both 40 and 80 cm depths (WL and SP monitoring points), the average standard deviation of soil water content at all locations varied from 0.05 to 0.07, while CV varied from 0.15 to 0.21. Although differences in slope have been determined, preliminary results suggest that slope does not have a lot of impact on the variability of the SWC, which is consistent with the similar research where it was shown that soil water retention in slopes was mostly related to the soil properties [5].

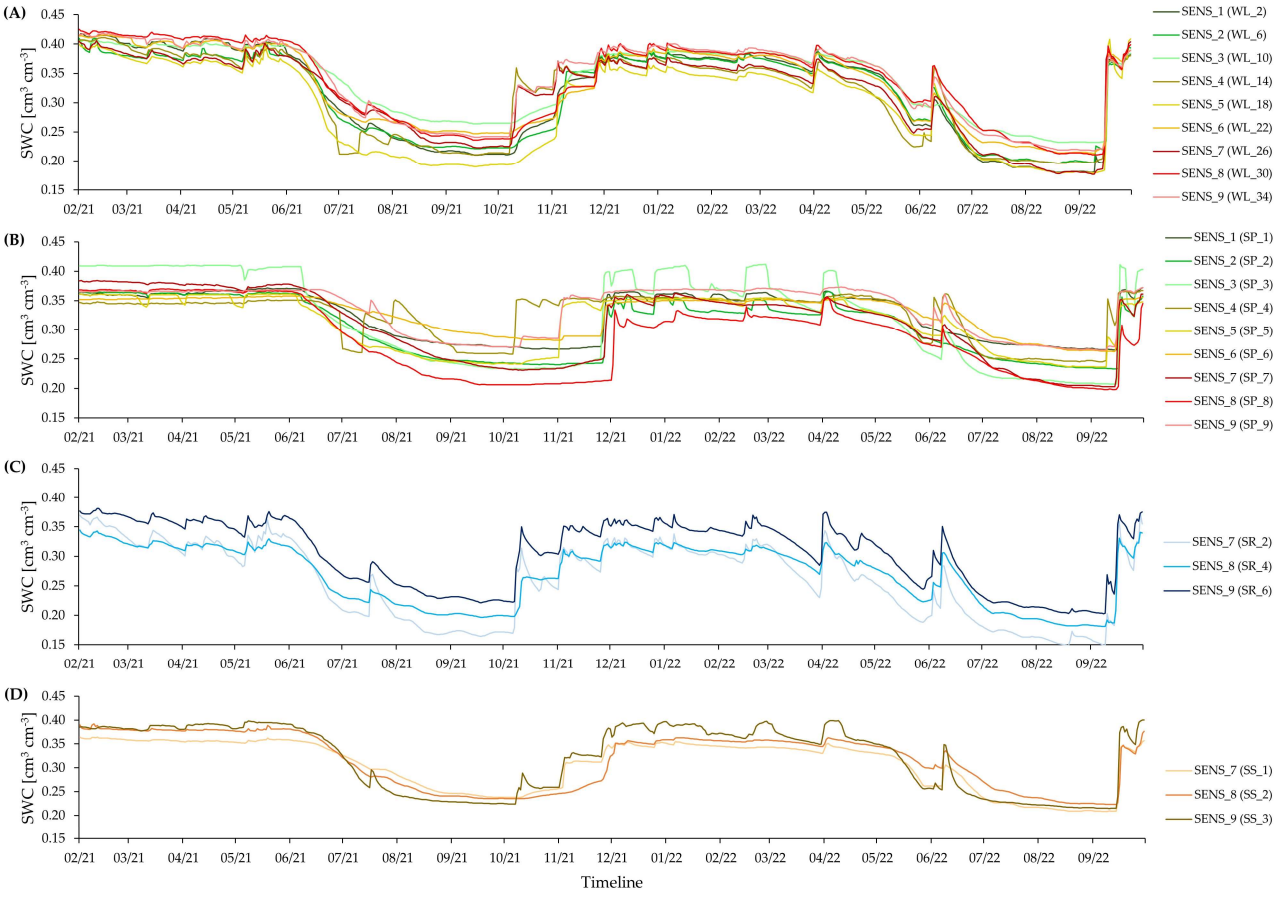

Figure 5. Variation of soil water content (SWC) in different positions close to (**A**) wick lysimeters; (**B**) suction cups; (**C**) surface runoff; (**D**) subsurface runoff.

Table 1. Basic statistical parameters related to the soil water content (SWC) in 24 monitoring points.

Monitoring Point	Average	Median	Maximum	Minimum	SD	CV
SR_2	0.26	0.28	0.37	0.15	0.06	0.25
SR_4	0.27	0.29	0.34	0.18	0.05	0.19
SR_6	0.31	0.33	0.38	0.20	0.06	0.18
SS_1	0.31	0.33	0.36	0.21	0.05	0.17
SS_2	0.32	0.34	0.39	0.22	0.06	0.18
SS_3	0.32	0.35	0.40	0.21	0.07	0.21
WL_2	0.32	0.35	0.42	0.18	0.08	0.25
WL_6	0.31	0.35	0.41	0.20	0.07	0.23
WL_10	0.34	0.37	0.41	0.23	0.06	0.17
WL_14	0.31	0.34	0.41	0.20	0.07	0.23
WL_18	0.29	0.33	0.41	0.18	0.07	0.25
WL_22	0.33	0.35	0.42	0.21	0.07	0.21
WL_26	0.31	0.34	0.41	0.18	0.07	0.21
WL_30	0.34	0.36	0.43	0.21	0.07	0.21
WL_34	0.34	0.37	0.42	0.22	0.07	0.20
SP_1	0.32	0.35	0.37	0.27	0.04	0.13
SP_2	0.30	0.33	0.37	0.23	0.05	0.16
SP_3	0.32	0.33	0.41	0.21	0.08	0.24
SP_4	0.33	0.35	0.37	0.25	0.04	0.12
SP_5	0.31	0.34	0.36	0.24	0.05	0.15
SP_6	0.33	0.35	0.36	0.26	0.03	0.10
SP_7	0.31	0.33	0.38	0.20	0.06	0.19
SP_8	0.29	0.30	0.37	0.20	0.06	0.21
SP_9	0.34	0.36	0.37	0.27	0.04	0.12

Granulometric composition at three depths in all nine locations, as well as values of C_{org}, are presented in Figure 6. In general, results showed that silt fraction is dominant at all positions, that sand has the highest average occurrence in the backslope and goes up to a maximum of 19%, and that clay content varies from 14% to 40%. C_{org} shows a similar trend in all locations, i.e., a decrease with depth, with the highest average values in the footslope. As previously mentioned, values of bulk density are presented in detail in Krevh et al. [59]. In this research, only average values of bulk density to a depth of 40 cm were used for the correlation analysis and interpretation purposes. Values of bulk density varied from 1.46 g/cm^3 to 1.59 g/cm^3, with the highest average values in the backslope and smallest in the hilltop.

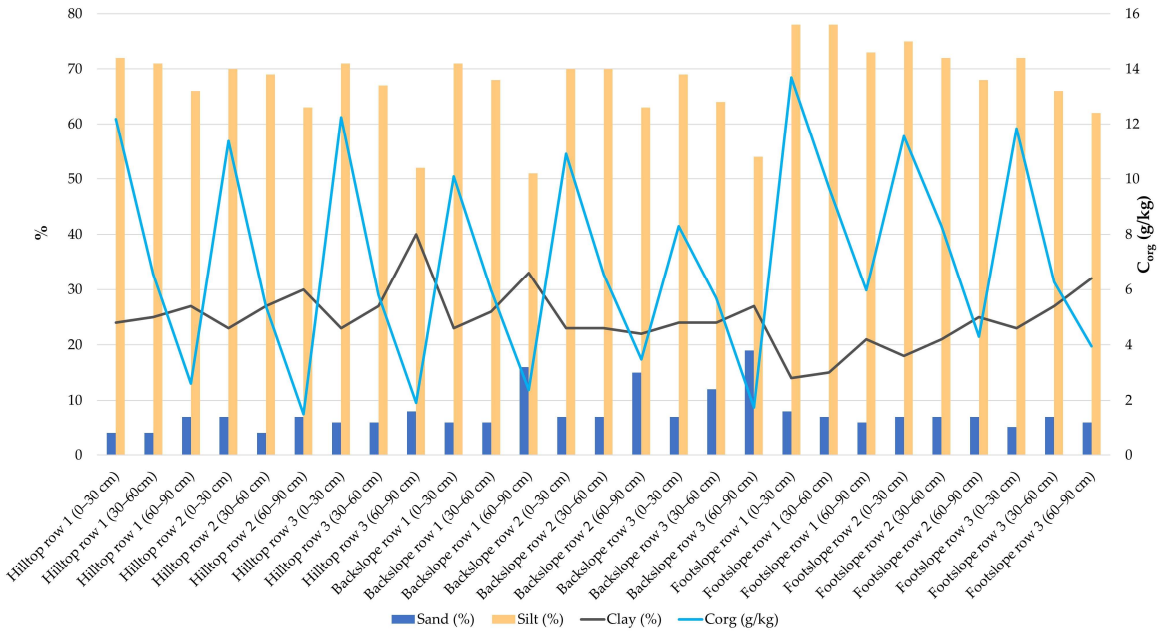

Figure 6. Granulometric composition and C_{org} in the observed vineyard.

3.3. Isotopic Composition and Water Mixing in the Hillslope Vineyard

Stable isotopes of oxygen and hydrogen from the precipitation and soil water are presented in Figure 7, while their variability can be additionally seen in Figure 8, where boxplots for δ^2H, $\delta^{18}O$ and d-excess are shown. The slope of the LMWL line is similar to the LMWL Zagreb [73] and LMWL Velika Gorica [53], which is expected due to the small distance between all three monitoring points.

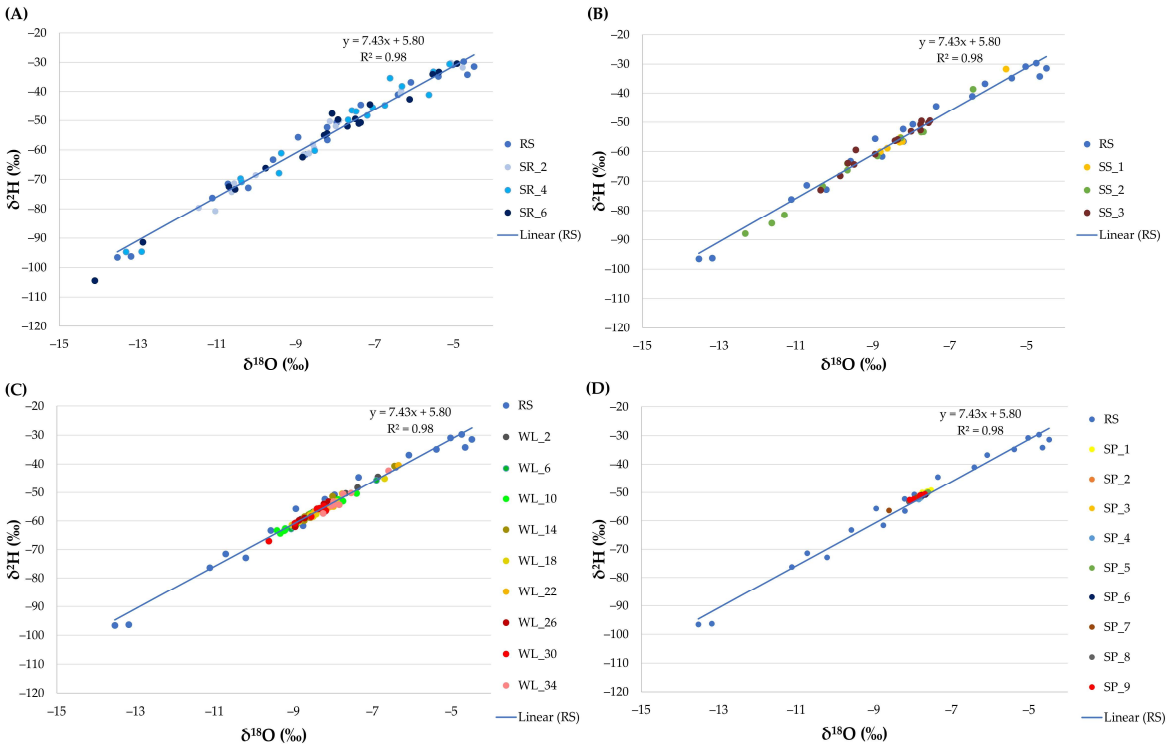

Figure 7. Comparison of isotopic composition of soil water with precipitation. (**A**) surface runoff (20 m depth); (**B**) subsurface runoff (60 cm depth); (**C**) wick lysimeters (40 cm depth); (**D**) suction cups (100 cm depth).

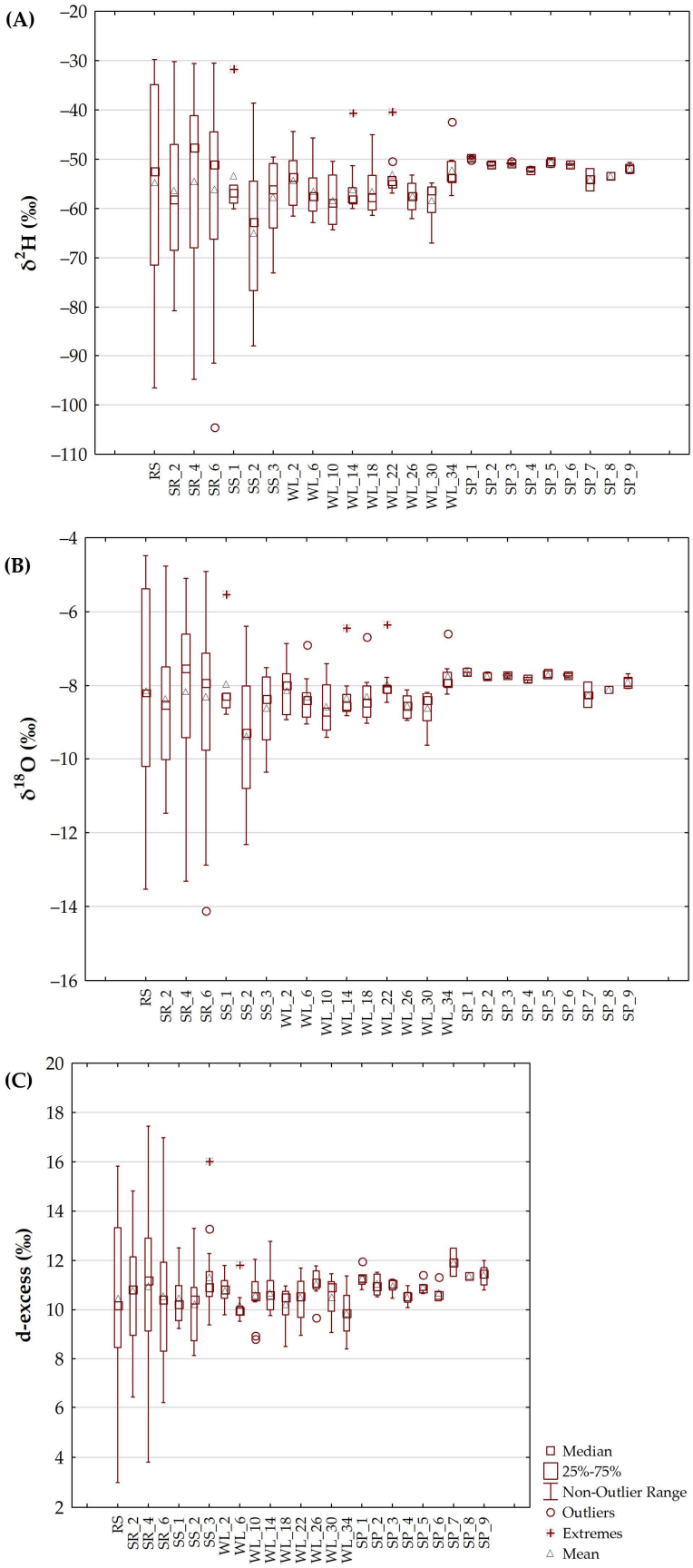

Figure 8. Variation of isotopic composition of soil water and precipitation. (**A**) δ^2H; (**B**) $\delta^{18}O$; (**C**) d-excess.

In Figure 7a, results suggested a similar isotopic pattern between the precipitation and surface runoff, which is reasonable to expect due to soil water which is captured in shallowest depth (20 cm). Values of δ^2H of the surface runoff mostly varied from −40‰ to −70‰, while $\delta^{18}O$ values in general varied from −7‰ to −10‰. D-excess values varied from 8‰ to 13‰ (Figures 7a and 8). As shown in Figure 7b, the isotopic signature of subsurface runoff also follows the LMWL, but, in Figure 7b, it can be clearly seen that the variability in the monitoring point SS_1, also located in the northwestern part of the footslope, was much lower with respect to the other two points. Subsurface runoff showed an isotopic signature mostly between −50‰ and −75‰, and between −8‰ and −11‰ for δ^2H and $\delta^{18}O$, respectively. D-excess, in most cases, varied from 9 to 11‰. In general, results suggested smaller variability in the northwestern part of the footslope in monitoring point SR_2 at 20 cm depth and SS_1 at 60 cm depth. There are numerous factors that can present a possible reason for that. Firstly, it is possible that, in this part of the vineyard, C_{org} has big influence on water flow, due to the determined highest values at all three depths (Figure 6). It has been shown that soil organic carbon can enhance permeability and water availability [13], as well as enhance hydraulic conductivity by improving aggregate porosity and stability [12–15]. However, in this location, except for the highest values of C_{org}, there is the highest average value of silt and lowest average value of clay (if all data from the whole vineyard are considered). The lowest share of clay could enable faster flow, in which less water could be captured with monitoring equipment and, in the end, generate less variation in the isotopic signature. This corresponds to the lowest average SWC for SR_2 and SS_1, which can be seen in Table 1, in comparison with other monitoring points which capture surface and subsurface flow. Furthermore, this also corresponds to the fact that, in the positions SR_2 and SS_1, much less volume has been captured (Figure 4). Additionally, it has been shown that footslope can have a deeper loose layer compared to the hilltop [8], which can cause heterogeneity and influence soil water dynamics. In this case, it is very interesting to see that, in the northwestern part of the footslope, there are the lowest values of bulk density in the first 40 cm depth, and the highest in the deepest parts. On the other two points in the footslope, values of bulk density are totally opposite with depth, as shown by Krevh et al. [59]. In the end, the influence of the slope of the vineyard on the surface and subsurface flow should not be neglected, which is from the northwest to southeast (Figure 1), although results from this study indicate that slope does not have a lot of impact on the variability of the soil water content, which corresponds to previous research where it was shown that the retention of soil water on the slope is more influenced by soil properties [5].

Isotopic signature from wick lysimeters follows the LMWL but shows much less variability than surface and subsurface runoff (Figure 7c). Values of δ^2H and $\delta^{18}O$ varied from approximately −50‰ to −60‰ and −8‰ to −9‰, respectively. D-excess values in general varied from 10‰ to 11‰. The smallest variation, within the limit of the precision of the instrument, can be seen for the isotopic signature of soil water from the suction probes (Figure 7d). This is expected because they are capturing soil water at 100 cm depth, and it is consistent with, in most cases, the lowest SWC variation at sensors located at 80 cm depth, as shown in Figure 5 and Table 1. Average and median δ^2H values of all analyses (n = 53) were −51.1‰ and −51.00‰, respectively, while the average and median of $\delta^{18}O$ value were −7.77‰ and −7.74‰. D-excess values, in almost all cases, varied from 10‰ to 12‰. In general, d-excess values from all water samples, especially those related to the soil water, suggest that evaporation did not have a significant impact on the isotopic composition. Although very similar, in Figure 8 it can be clearly seen that in the footslope isotopic signature shows slightly higher variation (SP_7, SP_8, and SP_9). All results together suggest that soil water from the suction probes presents mostly non-mobile water, probably associated with older precipitation and/or bulk water, and not related to the recent precipitation, i.e., precipitation which fell within the investigated time period. It must be emphasized that these kinds of instruments are usually used for sampling mobile water, while, for the purpose of sampling bulk soil water methods

such as cryogenic vacuum extraction [74,75] and other laboratory or in situ techniques are used [76,77]. However, increased intention related to the differentiation between sampling of bulk and mobile water has been pronounced in recent research [33], as well as the necessity to explore differences between their isotopic signatures [78]. Within this research, it is also not clear whether the soil water captured by suction probes presents bulk water or older precipitation, or a mixture of water between them, which points to the need for more detailed research in future. On the other side, it is clear that recent precipitation did not have a lot of influence on the isotopic composition of soil water at 100 cm depth, at least in the observed time period, which indicates that water mixing mainly took place in the shallower parts of the vineyard.

In order to define precipitation fractions in soil water at different monitoring points, a two-component mixing model using $\delta^{18}O$ values has been applied. It was performed in a way that soil water captured from suction probes was defined as non-mobile water, while precipitation was the only input, i.e., the only source of recharge. As mentioned before, not all months were included in the mixing model due to lack of data. In the end, it was decided to use only months where at least half of the monitoring points, i.e., 12 locations, had determined isotopic composition. These months generally coincide with the period from September to May, for which most of the soil water isotopic composition was available (191 of 228). For the $\delta^{18}O$ value of the precipitation, the average value from the used months was calculated, i.e., −9.65‰. All data from suction probes have been checked for outliers and extreme values using a box-plot, which resulted in the exclusion of five values and the final average value of −7.73‰. For surface runoff, subsurface runoff, and wick lysimeters, the average values from the selected time period have been used for each location separately (Table 2). Results suggest different values of precipitation fraction within the soil water. The highest values can be seen for the surface runoff, as expected, from approximately 80% up to more than 97%. Precipitation fraction within subsurface runoff varies greatly, from about 9% in the northwestern part of the footslope up to almost 98% percent in the central part of the footslope, which suggests a very heterogeneous area as well as different influences of soil physicochemical parameters and erosion processes on the water flow. Precipitation infiltration to wick lysimeters also shows different patterns within the vineyard, from fractions of more than 1% up to almost 47%. In general, a very small precipitation fraction can be seen at the backslope of the vineyard, which is especially related to the point WL_22, which had the smallest average values of C_{org} as well as the highest share of sand. An additional very interesting isotopic signature has been observed in point WL_34, located in the southeastern part of the footslope. Within this point, the smallest precipitation fraction is observed, totally different from the other two points in the footslope, which suggests much higher precipitation infiltration, i.e., about 45%. The possible reasons for that are related to the highest clay content of the footslope when observing first 30 cm depth, as well as the slightly higher average bulk density in first 40 cm depth. Previous results showed that proportion of clays in soil determines the occurrence of soil water repellency [79] and that soils with a predominance of clay have stronger water repellency than coarse-textured soils [80].

Results related to the estimation of the precipitation fractions captured by wick lysimeters suggested great variability and dependence to different physicochemical parameters in different parts of the vineyard, which is expected due to heterogeneity and more and less pronounced erosion, especially in the footslope part. In order to statistically define the relationship between precipitation infiltration and physicochemical parameters, correlation analysis has been performed using values for first 30 cm depth, which are related to the granulometric composition, and C_{org}, while average bulk density values for first 40 cm depth were used based on the HYPROP-FIT estimation presented in Krevh et al. [59]. In Table 3, correlation matrix is presented, while statistically significant results are marked in red ($\alpha = 0.05$). Although not statistically significant, it can be clearly seen that precipitation infiltration is positively correlated with C_{org}, sand and silt, and negatively correlated with clay content and bulk density. This also implies that precipitation infiltration depends on

the joint influence of the different soil parameters, which quantification should be one of the focuses of the future research. Statistically significant negative correlation was observed between silt and clay content, while statistically positive significant correlation was related to the connection between C_{org} and silt content. Results also showed that C_{org} in this case is not positively correlated with the clay content. Although maybe not that common, research conducted in arid and semi-arid regions has shown that fine silt can contribute more organic carbon then clay when its proportion is relatively higher than clay [81], which can also be the case in this research.

Table 2. Results of two-component mixing model.

Monitoring Point	Average $\delta^{18}O$ (‰)	Precipitation Fraction in Soil Water (%)
SR_2	−9.27	80.48
SR_4	−9.36	84.83
SR_6	−9.60	97.50
SS_1	−7.90	8.88
SS_2	−9.61	97.97
SS_3	−8.69	50.24
WL_2	−8.15	21.98
WL_6	−8.33	31.55
WL_10	−8.63	46.98
WL_14	−8.31	30.45
WL_18	−8.29	29.16
WL_22	−7.91	9.84
WL_26	−8.57	44.11
WL_30	−8.62	46.29
WL_34	−7.75	1.16

Table 3. Correlation matrices between precipitation fraction in soil water and soil physicochemical parameters.

Parameter	Precipitation Fraction (%)	C_{org} (g/kg)	Sand (%)	Silt (%)	Clay (%)	Bulk Density (g/cm^3)
Precipitation fraction (%)	1.00	-	-	-	-	-
C_{org} (g/kg)	0.47	1.00	-	-	-	-
Sand (%)	0.46	−0.05	1.00	-	-	-
Silt (%)	0.48	0.73	0.29	1.00	-	-
Clay (%)	−0.57	−0.59	−0.60	−0.94	1.00	-
Bulk density (g/cm^3)	−0.55	−0.64	−0.20	−0.35	0.37	1.00

Furthermore, it must be emphasized that long-term monitoring has to be established in order to achieve more reliable results. This is especially related to the sampling of soil water in the summer months, which was not possible in all monitoring points within the investigated period. Furthermore, for a more detailed statistical inspection of all observed parameters, as well as to define their relationship under different hydro-meteorological conditions, additional data is necessary [82–88]. In addition to long-term data collection, future research should be focused to the development of water flow and transport models,

evaluation of seasonal patterns of different hydrometeorological variables, and definition of the isotopic difference between mobile, non-mobile, and bulk water.

4. Conclusions

This paper presents research related to the estimation of precipitation fractions in the soil water at the SUPREHILL CZO, located in the City of Zagreb, Croatia. It is a sloped vineyard where the monitoring of soil water isotopic composition was conducted in 24 points at 4 depths. It has been shown that soil water isotopic composition from all monitoring points coincides with the calculated LMWL, with almost no variability at 100 cm depth, which is consistent with the smallest variation of SWC. This suggests the existence of non-mobile soil water, on which the precipitation influence can not be seen in the observed period, and that most of the water mixing occurs in first 100 cm depth. Results also suggest the existence of heterogeneity, uneven erosion processes in the footslope, and different infiltration patterns. Fractions of precipitation in soil water varied depending on the depth and position in the vineyard, from approximately 1% up to 98%, where more precipitation fraction can be seen in the surface and subsurface runoff. Statistical analysis and detailed evaluation of the physicochemical parameters and isotopic composition of soil water captured by wick lysimeters has shown that C_{org} content is, in general, related to the silt fraction, while the first results indicate that infiltration patterns are dependent on the common influence of all observed physicochemical properties. Furthermore, it has been shown that captured water volumes varied significantly with respect to the position in the vineyard, sampling depth, and used equipment, while sampling of soil water in summer months was challenging due to dry conditions. However, monitoring must be continued in order to achieve more reliable results, while future research should be focused on the development of a soil water flow model calibrated using stable isotopes of water, an evaluation of the differences in the isotopic signature of mobile, non-mobile, and bulk water, as well as on the examination of the relationship between the observed parameters in different hydrometeorological conditions.

Author Contributions: Conceptualization, Z.K., V.K., L.F. and V.F.; methodology, Z.K., V.K. and V.F.; software, Z.K., V.K., J.D. and B.-I.B.; formal analysis, Z.K., V.K., J.D. and B.-I.B.; investigation, Z.K., V.K., L.F., J.D. and V.F.; resources, Z.K., L.F. and V.F.; data curation, Z.K. and V.K.; writing—original draft preparation, Z.K.; writing—review and editing, V.K., L.F., J.D., B.-I.B. and V.F.; visualization, Z.K., V.K. and B.-I.B.; supervision, L.F. and V.F.; funding acquisition, L.F. and V.F. All authors have read and agreed to the published version of the manuscript.

Funding: This research was funded by the Croatian Science Foundation, grant number UIP-2019-04-5409, project: "Subsurface preferential transport processes in agricultural hillslope soils–SUPREHILL".

Institutional Review Board Statement: Not applicable.

Informed Consent Statement: Not applicable.

Data Availability Statement: The data presented in this study are available on request from the corresponding author. The data are not publicly available due to ongoing research publications and PhD thesis.

Acknowledgments: We want to thank the International Atomic Energy Agency (IAEA) for providing technical support (laser instrument and training) in IAEA TC Project CRO7001 (Isotope Investigation of the Groundwater–Surface Water Interaction at the Well Field Kosnica in the Area of the City of Zagreb).

Conflicts of Interest: The authors declare no conflict of interest.

References

1. Fan, Y.; Clark, M.; Lawrence, D.M.; Swenson, S.; Band, L.E.; Brantley, S.L.; Brooks, P.D.; Dietrich, W.E.; Flores, A.; Grant, G.; et al. Hillslope Hydrology in Global Change Research and Earth System Modeling. *Water Resour. Res.* **2019**, *55*, 1737–1772. [CrossRef]
2. Filipović, V.; Coquet, Y.; Gerke, H.H. Representation of Plot-Scale Soil Heterogeneity in Dual-Domain Effective Flow and Transport Models with Mass Exchange. *Vadose Zone J.* **2019**, *18*, 1–14. [CrossRef]

3. Filipović, V.; Defterdarović, J.; Šimůnek, J.; Filipović, L.; Ondrašek, G.; Romić, D.; Bogunović, I.; Mustać, I.; Ćurić, J.; Kodešová, R. Estimation of vineyard soil structure and preferential flow using dye tracer, X-ray tomography, and numerical simulations. *Geoderma* **2020**, *380*, 114699. [CrossRef]
4. Nimmo, J.R. The processes of preferential flow in the unsaturated zone. *Soil Sci. Soc. Am. J.* **2021**, *85*, 1–27. [CrossRef]
5. Magdić, I.; Safner, T.; Rubinić, V.; Rutić, F.; Husnjak, S.; Filipović, V. Effect of slope position on soil properties and soil moisture regime of Stagnosol in the vineyard. *J. Hydrol. Hydromech.* **2022**, *70*, 62–73. [CrossRef]
6. Apollonio, C.; Petroselli, A.; Tauro, F.; Cecconi, M.; Biscarini, C.; Zarotti, C.; Grimaldi, S. Hillslope erosion mitigation: An experimental proof of a nature-based solution. *Sustainability* **2021**, *13*, 6058. [CrossRef]
7. Nikodem, A.; Kodešová, R.; Fér, M.; Klement, A. Using scaling factors for characterizing spatial and temporal variability of soil hydraulic properties of topsoils in areas heavily affected by soil erosion. *J. Hydrol.* **2021**, *593*, 125897. [CrossRef]
8. Filipović, V.; Defterdarović, J.; Krevh, V.; Filipović, L.; Ondrašek, G.; Kranjčec, F.; Magdić, I.; Rubinić, V.; Stipičević, S.; Mustać, I.; et al. Estimation of stagnosol hydraulic properties and water flow using uni-and bimodal porosity models in erosion-affected hillslope vineyard soils. *Agronomy* **2022**, *12*, 33. [CrossRef]
9. Gazis, C.; Feng, X. A stable isotope study of soil water: Evidence for mixing and preferential flow paths. *Geoderma* **2004**, *119*, 97–111. [CrossRef]
10. Holden, J. Infiltration/Capacity/Rates. *Water Encycl.* **2005**, *5*, 212–214.
11. Mao, J.; Nierop, K.G.J.; Dekker, S.C.; Dekker, L.W.; Chen, B. Understanding the mechanisms of soil water repellency from nanoscale to ecosystem scale: A review. *J. Soils Sediments* **2019**, *19*, 171–185. [CrossRef]
12. Mahmoodabadi, M.; Ahmadbeygi, B. Dry and water-stable aggregates in different cultivation systems of arid region soils. *Arabian J. Geosci.* **2013**, *6*, 2997–3002. [CrossRef]
13. Cassinari, C.; Manfredi, P.; Giupponi, L.; Trevisan, M.; Piccini, C. Relationship between hydraulic properties and plant coverage of the closed-landfill soils in Piacenza (Po Valley, Italy). *Solid Earth* **2015**, *6*, 929–943. [CrossRef]
14. Eibisch, N.; Durner, W.; Bechtold, M.; Fuss, R.; Mikutta, R.; Woche, S.K.; Helfrich, M. Does water repellency of pyrochars and hydrochars counter their positive effects on soil hydraulic properties? *Geoderma* **2015**, *245–246*, 31–39. [CrossRef]
15. Yazdanpanah, N.; Mahmoodabadi, M.; Cerdà, A. The impact of organic amendments on soil hydrology, structure and microbial respiration in semiarid lands. *Geoderma* **2016**, *266*, 58–65. [CrossRef]
16. Grayson, R.B.; Western, A.W.; Chiew, F.H.S.; Blöschl, G. Preferred states in spatial soil moisture patterns: Local and nonlocal controls. *Water Resour. Res.* **1997**, *33*, 2897–2908. [CrossRef]
17. Stieglitz, M.; Shaman, J.; McNamara, J.; Engel, V.; Shanley, J.; Kling, G.W. An approach to understanding hydrologic connectivity on the hillslope and the implications for nutrient transport. *Glob. Biogeochem. Cycles* **2003**, *17*, 1–15. [CrossRef]
18. McNamara, J.P.; Chandler, D.; Seyfried, M.; Achet, S. Soil moisture states, lateral flow, and streamflow generation in a semi-arid, snowmelt-driven catchment. *Hydrol. Process.* **2005**, *19*, 4023–4038. [CrossRef]
19. Dusek, J.; Dohnal, M.; Snehota, M.; Sobotkova, M.; Ray, C.; Vogel, T. Transport of bromide and pesticides through an undisturbed soil column: A modeling study with global optimization analysis. *J. Contam. Hydrol.* **2015**, *175–176*, 1–16. [CrossRef]
20. Pietrzak, D.; Kania, J.; Kmiecik, E.; Wator, K. Identification of transport parameters of chlorides in different soils on the basis of column studies. *Geologos* **2019**, *25*, 225–229. [CrossRef]
21. Beck-Broichsitter, S.; Gerriets, M.R.; Gerke, H.H.; Sobotkova, M.; Dusek, J.; Dohrmann, R.; Horn, R. Brilliant Blue sorption characteristics of clay-organic aggregate coatings from Bt horizons. *Soil Tillage Res.* **2020**, *201*, 104635. [CrossRef]
22. Knighton, J.; Saia, S.M.; Morris, C.K.; Archiblad, J.A.; Walter, M.T. Ecohydrologic considerations for modeling of stable water isotopes in a small intermittent watershed. *Hydrol. Process.* **2017**, *31*, 2438–2452. [CrossRef]
23. Rothfuss, Y.; Javaux, M. Reviews and syntheses: Isotopic approaches to quantify root water uptake: A review and comparison of methods. *Biogeosciences* **2017**, *14*, 2199–2224. [CrossRef]
24. Barbecot, F.; Guillon, S.; Pili, E.; Larocque, M.; Gibert-Brunet, E.; Hélie, J.-F.; Noret, A.; Plain, C.; Schneider, V.; Mattei, A.; et al. Using water stable isotopes in the unsaturated zone to quantify recharge in two contrasted infiltration regimes. *Vadose Zone J.* **2018**, *17*, 1–13. [CrossRef]
25. Jin, K.; Rao, W.; Wang, S.; Zhang, W.; Zheng, F.; Li, T.; Lu, Y.; Zhang, Q. Stable isotopes ($\delta^{18}O$ and $\delta^{2}H$) and chemical characteristics of soil solution in the unsaturated zone of an arid desert. *J. Radioanal. Nucl. Chem.* **2012**, *330*, 367–380. [CrossRef]
26. Zhu, G.; Yong, L.; Zhao, X.; Liu, Y.; Zhang, Z.; Xu, Y.; Sun, Z.; Sang, L.; Wang, L. Evaporation, infiltration and storage of soil water in different vegetation zones in the Qilian Mountains: A stable isotope perspective. *Hydrol. Earth Syst. Sci.* **2022**, *26*, 3771–3784. [CrossRef]
27. Dusek, J.; Vogel, T.; Dohnal, M.; Barth, J.A.; Sanda, M.; Marx, A.; Jankovec, J. Dynamics of dissolved organic carbon in hillslope discharge: Modeling and challenges. *J. Hydrol.* **2017**, *546*, 309–325. [CrossRef]
28. Dusek, J.; Vogel, T. Hillslope hydrograph separation: The effects of variable isotopic signatures and hydrodynamic mixing in macroporous soil. *J. Hydrol.* **2018**, *563*, 446–459. [CrossRef]
29. Song, X.; Wang, S.; Xiao, G.; Wang, Z.; Liu, X.; Wang, P. A study of soil water movement combining soil water potential with stable isotopes at two sites of shallow groundwater areas in the North China Plain. *Hydrol. Process.* **2009**, *23*, 1376–1388. [CrossRef]
30. Peralta-Tapia, A.; Sponseller, R.A.; Tetzlaff, D.; Soulsby, C.; Laudon, H. Connecting precipitation inputs and soil flow pathways to stream water in contrasting boreal catchments. *Hydrol. Process.* **2015**, *29*, 3546–3555. [CrossRef]

31. Kelln, C.; Barbour, L.; Qualizza, C. Preferential flow in a reclamation cover: Hydrological and geochemical response. J. Geotech. *Geoenviron. Eng.* **2007**, *133*, 1277–1289. [CrossRef]
32. Sprenger, M.; Leistert, H.; Gimbel, K.; Weiler, M. Illuminating hydrological processes at the soil-vegetation-atmosphere interface with water stable isotopes. *Rev. Geophys.* **2016**, *54*, 674–704. [CrossRef]
33. Sprenger, M.; Tetzlaff, D.; Buttle, J.; Laudon, H.; Leistert, H.; Mitchell, C.P.J.; Snelgrove, J.; Weiler, M.; Soulsby, C. Measuring and modeling stable isotopes of mobile and bulk soil water. *Vadose Zone J.* **2018**, *17*, 1–18. [CrossRef]
34. Kendall, C.; McDonnell, J.J. (Eds.) *Isotope Tracers in Catchment Hydrology*; Elsevier: Amsterdam, The Netherlands, 2012.
35. Goldsmith, G.R.; Muñoz-Villers, L.E.; Holwerda, F.; McDonnell, J.J.; Asbjornsen, H.; Dawson, T.E. Stable isotopes reveal linkages among ecohydrological processes in a seasonally dry tropical montane cloud forest. *Ecohydrology* **2012**, *5*, 779–790. [CrossRef]
36. Good, S.P.; Noone, D.; Bowen, G. Hydrologic connectivity constrains partitioning of global terrestrial water fluxes. *Science* **2015**, *349*, 175–177. [CrossRef]
37. Sprenger, M.; Llorens, P.; Cayuela, C.; Gallart, F.; Latron, J. Mechanisms of consistently disjunct soil water pools over (pore) space and time. *Hydrol. Earth Syst. Sci.* **2019**, *23*, 2751–2762. [CrossRef]
38. Sprenger, M.; Stumpp, C.; Weiler, M.; Aeschbach, W.; Allen, S.; Benettin, P.; Dubbert, M.; Hartmann, A.; Hrachowitz, M.; Kirchner, J.W.; et al. The demographics of water: A review of water ages in the critical zone. *Rev. Geophys.* **2019**, *57*, 800–834. [CrossRef]
39. Wang, H.; Jin, J.; Cui1, B.; Si, B.; Ma, X.; Wen, M. Technical note: Evaporating water is different from bulk soil water in δ^2H and δ^{18}O and has implications for evaporation calculation. *Hydrol. Earth Syst. Sci.* **2021**, *25*, 5399–5413. [CrossRef]
40. Oerter, E.; Finstad, K.; Schaefer, J.; Goldsmith, G.R.; Dawson, T.; Amundson, R. Oxygen isotope fractionation effects in soil water via interaction with cations (Mg, Ca, K, Na) adsorbed to phyllosilicate clay minerals. *J. Hydrol.* **2014**, *515*, 1–9. [CrossRef]
41. Gaj, M.; Kaufhold, S.; Koeniger, P.; Beyer, M.; Weiler, M.; Himmelsbach, T. Mineral mediated isotope fractionation of soil water. *Rapid Commun. Mass Spectrom.* **2017**, *31*, 269–280. [CrossRef]
42. Gaj, M.; McDonnell, J.J. Possible soil tension controls on the isotopic equilibrium fractionation factor for evaporation from soil. *Hydrol. Process.* **2019**, *33*, 1629–1634. [CrossRef]
43. Thielemann, L.; Gerjets, R.; Dyckmans, J. Effects of soilbound water exchange on the recovery of spike water by cryogenic water extraction. *Rapid Commun. Mass Spectrom.* **2019**, *33*, 405–410. [CrossRef]
44. Orlowski, N.; Breuer, L. Sampling soil water along the pF curve for δ^2H and δ^{18}O analysis. *Hydrol. Process.* **2020**, *34*, 4959–4972. [CrossRef]
45. Posavec, K.; Vukojević, P.; Ratkaj, M.; Bedeniković, T. Cross-correlation modelling of surface water-groundwater interaction using the Excel spreadsheet application. *Rud. -Geološko-Naft. Zb.* **2017**, *32*, 25–32. [CrossRef]
46. Vujević, M.; Posavec, K. Identification of Groundwater Level Decline in the Zagreb and Samobor-Zapresic Aquifers since the Sixties of the Twentieth Century. *Rud. -Geološko-Naft. Zb.* **2018**, *33*, 55–64. [CrossRef]
47. Parlov, J.; Kovač, Z.; Nakić, Z.; Barešić, J. Using water stable isotopes for identifying groundwater recharge sources of the unconfined alluvial Zagreb aquifer (Croatia). *Water* **2019**, *11*, 2177. [CrossRef]
48. Barešić, J.; Parlov, J.; Kovač, Z.; Sironić, A. Use of nuclear power plant released tritium as groundwater tracer. *Rud. -Geološko-Naft. Zb.* **2020**, *35*, 25–34. [CrossRef]
49. Kovač, Z.; Barešić, J.; Parlov, J.; Sironić, A. Impact of Hydrological Conditions on the Isotopic Composition of the Sava River in the Area of the Zagreb Aquifer. *Water* **2022**, *14*, 2263. [CrossRef]
50. Ružičić, S.; Mileusnić, M.; Posavec, K.; Nakić, Z.; Durn, G.; Filipović, V. Water flow and solute transport model of potentially toxic elements through unsaturated zone at regional wellfield Kosnica. *Hydrol. Process.* **2016**, *30*, 4113–4124. [CrossRef]
51. Ružičić, S.; Kovač, Z.; Tumara, D. Physical and chemical properties in relation to soil permeability in the area of the Velika Gorica well field. *Rud. -Geološko-Naft. Zb.* **2018**, *33*, 73–81. [CrossRef]
52. Kovač, Z.; Ružičić, S.; Rubinić, V.; Nakić, Z.; Sertić, M. Sorption of cadmium, zinc and copper in dominant soils of Zagreb aquifer system, Croatia. *Geologia Croat.* **2022**, *75*, 177–188. [CrossRef]
53. Ružičić, S.; Balaž, B.-I.; Kovač, Z.; Filipović, L.; Nakić, Z.; Kopić, J. Nickel and Chromium Origin in Fluvisols of the Petruševec Well Field, Zagreb Aquifer. *Environments* **2022**, *9*, 154. [CrossRef]
54. Kovač, Z.; Bačani, L.; Ružičić, S.; Parlov, J.; Posavec, K.; Buškulić, P. Using Water Stable Isotopes and Cross-Correlation Analysis to Characterize Infiltration of Precipitation through Unsaturated Zone at the Velika Gorica Site of Zagreb Aquifer. *J. Hydrol. Eng.* **2023**, *28*, 04023003. [CrossRef]
55. Kovač, Z.; Krevh, V.; Filipović, L.; Defterdarović, J.; Buškulić, P.; Han, L.; Filipović, V. Utilizing Stable Water Isotopes (δ^2H and δ^{18}O) To Study Soil-Water Origin in Sloped Vineyard: First Results. *Rudarsko-geološko-naftni zbornik* **2022**, *37*, 1–14. [CrossRef]
56. Allen, R. Penman-Monteith equation. In *Encyclopedia of Soils in the Environment*; Hillel, D., Rosenzweig, C., Powlson, D., Scow, K., Singer, M., Sparks, D., Eds.; Academic Press: Cambridge, MA, USA, 2004; pp. 180–187, 570p.
57. *ISO 11277:2020*; Soil Quality—Determination of Particle Size Distribution in Mineral Soil Material–Method by sieving and Sedimentation. ISO: Geneva, Switzerland, 2020. Available online: https://www.iso.org/standard/69496.html (accessed on 6 February 2022).
58. *ISO 14235:1998*; Soil Quality—Determination of Organic Carbon by Sulfochromic Oxidation. ISO: Geneva, Switzerland, 1998. Available online: https://www.iso.org/standard/23140.html (accessed on 11 November 2022).

59. Krevh, V.; Groh, J.; Weihermüller, L.; Filipović, L.; Defterdarović, J.; Kovač, Z.; Magdić, I.; Lazarević, B.; Baumgartl, T.; Filipović, V. Investigation of hillslope vineyard soil water dynamics using field measurements and numerical modeling. *Water* **2023**, *15*, 820. [CrossRef]
60. *USDA Soil Taxonomy: A Basic System of Soil Classification for Making and Interpreting Soil Surveys*; Soil Survey Staff, United States Department of Agriculture: Washington, DC, USA, 1999; 436p.
61. Lis, G.; Wassenaar, L.I.; Hendry, J. High-Precision Laser Spectroscopy D/H and 18O/16O Measurements of Microliter Natural Water Samples. *Anal. Chem.* **2008**, *80*, 287–293. [CrossRef]
62. Coplen, T.B.; Wassenaar, L.I. LIMS for Lasers for achieving long-term accuracy and precision of δ^2H, δ^{17}O, and δ^{18}O of waters using laser absorption spectrometry. *Rapid Commun. Mass Spectrom.* **2015**, *29*, 2122–2130. [CrossRef]
63. Rozanski, K.; Araguás-Araguás, L.; Gonfiantini, R. Isotopic patterns in modern global precipitation. *Geophys. Monogr.* **1993**, *78*, 1–36. [CrossRef]
64. Coplen, T.B. New guidelines for the reporting of stable hydrogen, carbon, and oxygen isotope ratio data. *Geochim. Cosmochim. Acta* **1996**, *60*, 3359–3360. [CrossRef]
65. Coplen, T.B.; Bohlke, J.K.; De Bievre, P.; Ding, T.; Holden, N.E.; Hopple, J.A.; Krouse, H.R.; Lamberty, A.; Peiser, P.S.; Revesz, K.; et al. Isotope-abundance variations of selected elements (IUPAC Technical Report). *Pure Appl. Chem.* **2002**, *74*, 1987–2017. [CrossRef]
66. Dansgaard, W. Stable isotopes in precipitation. *Tellus* **1964**, *16*, 436–468. [CrossRef]
67. Gröning, M.; Lutz, H.O.; Roller-Lutz, Z.; Kralik, M.; Gourcy, L.; Pöltenstein, L. A simple rain collector preventing water re-evaporation dedicated for δ^{18}O and δ^2H analysis of cumulative precipitation samples. *J. Hydrol.* **2012**, *448–449*, 195–200. [CrossRef]
68. Michelsen, N.; van Geldern, R.; Rossmann, Y.; Bauer, I.; Schulz, S.; Barth, J.A.C.; Schüth, C. Comparison of precipitation collectors used in isotope hydrology. *Chem. Geol.* **2018**, *488*, 171–179. [CrossRef]
69. Peng, T.R.; Wang, C.H.; Hsu, S.M.; Wang, G.S.; Su, T.W.; Lee, J.F. Identification of groundwater sources of a local-scale creep slope: Using environmental stable isotopes as tracers. *J. Hydrol.* **2010**, *381*, 151–157. [CrossRef]
70. Shahul Hameed, A.; Resmi, T.R.; Suraj, S.; Unnikrishnan Warrier, C.; Sudheesh, M.; Deshpande, R.D. Isotopic characterization and mass balance reveals groundwater recharge pattern in Chaliyar river basin, Kerala, India. *J. Hydrol. Reg. Stud.* **2015**, *4*, 48–58. [CrossRef]
71. Vrzel, J.; Kip Solomon, D.; Blaženka, Ž.; Ogrinc, N. The study of the interactions between groundwater and Sava River water in the Ljubljansko polje aquifer system (Slovenia). *J. Hydrol.* **2018**, *556*, 384–396. [CrossRef]
72. Croatian Meteorological and Hydrological Service. Available online: https://meteo.hr/klima.php?section=klima_pracenje&param=ocjena&el=msg_ocjena&MjesecSezona=godina&Godina=2021 (accessed on 12 January 2023).
73. Krajcar-Bronić, I.; Barešić, J.; Borković, D.; Sironić, A.; Lovrenčić Mikelić, I.; Vreča, P. Long-Term Isotope Records of Precipitation in Zagreb, Croatia. *Water* **2020**, *12*, 226. [CrossRef]
74. Koeniger, P.; Marshall, J.D.; Link, T.; Mulch, A. An inexpensive, fast, and reliable method for vacuum extraction of soil and plant water for stable isotope analyses by mass spectrometry. *Rapid Commun. Mass Spectrom.* **2011**, *25*, 3041–3048. [CrossRef]
75. Orlowski, N.; Frede, H.G.; Brüggemann, N.; Breuer, L. Validation and application of a cryogenic vacuum extraction system for soil and plant water extraction for isotope analysis. *J. Sens. Sens. Syst.* **2013**, *2*, 179–193. [CrossRef]
76. Wassenaar, L.; Hendry, M.; Chostner, V.; Lis, G. High resolution pore water δ^2H and δ^{18}O measurements by H_2O (liquid)–H_2O (vapor) equilibration laser spectroscopy. *Environ. Sci. Technol.* **2008**, *42*, 9262–9267. [CrossRef]
77. Volkmann, T.H.M.; Weiler, M. Continual in situ monitoring of pore water stable isotopes in the subsurface. *Hydrol. Earth Syst. Sci.* **2014**, *18*, 1819–1833. [CrossRef]
78. Newberry, S.L.; Prechsl, U.E.; Pace, M.; Kahmen, A. Tightly bound soil water introduces isotopic memory effects on mobile and extractable soil water pools. *Isot. Environ. Health Stud.* **2017**, *53*, 368–381. [CrossRef] [PubMed]
79. Kraemer, F.B.; Hallett, P.D.; Morrás, H.; Garibaldi, L.; Cosentino, D.; Duval, M.; Galantini, J. Soil stabilisation by water repellency under no-till management for soils with contrasting mineralogy and carbon quality. *Geoderma* **2019**, *355*, 113902. [CrossRef]
80. Vogelmann, E.S.; Reichert, J.M.; Reinert, D.J.; Mentges, M.I.; Vieira, D.A.; de Barros, C.A.P.; Fasinmirin, J.T. Water repellency in soils of humid subtropical climate of Rio Grande do Sul, Brazil. *Soil Tillage Res.* **2010**, *110*, 126–133. [CrossRef]
81. Mao, J.; Li, Y.; Zhang, J.; Zhang, K.; Ma, X.; Wang, G.; Fan, L. Organic carbon and silt determining subcritical water repellency and field capacity of soils in arid and semi-arid region. *Front. Environ. Sci.* **2022**, *10*, 13. [CrossRef]
82. Qin, W.; Chi, B.; Oenema, O. Long-Term Monitoring of Rainfed Wheat Yield and Soil Water at the Loess Plateau Reveals Low Water Use Efficiency. *PLoS ONE* **2013**, *8*, e78828. [CrossRef]
83. Haktanir, T.; Citakoglu, H.; Seckin, N. Regional frequency analyses of successive duration annual maximum rainfalls by L-moments method. *Hydrol. Sci. J.* **2016**, *61*, 647–648. [CrossRef]
84. Dinca, L.; Badea, O.; Guiman, G.; Braga, C.; Crisan, V.; Greavu, V.; Murariu, G.; Georgescu, L. Monitoring of soil moisture in Long-Term Ecological Research (LTER) sites of Romanian Carpathians. *Ann. For. Res.* **2018**, *61*, 171–188. [CrossRef]
85. Klotzsche, A.; Lärm, L.; Vanderborght, J.; Cai, G.; Morandage, S.; Zörner, M.; Vereecken, H.; van der Kruk, J. Monitoring soil water content using timelapse horizontal borehole GPR data at the field-plot scale. *Vadose Zone J.* **2019**, *18*, 190044. [CrossRef]
86. Citakoglu, H.; Demir, V. Developing numerical equality to regional intensity–duration–frequency curves using evolutionary algorithms and multi-gene genetic programming. *Acta Geophys.* **2022**, *71*, 469–488. [CrossRef]

87. Reyes-Hernández, M.F.; Castro-López, J.A.; Tarín, T.; Garatuza-Payán, J.; Encinas-Yépiz, D.H.; Yépez, E.A. A long-term dataset of stable isotopes in rainfall at the North American monsoon region in southern Sonora, Mexico. *Data Brief* **2022**, *45*, 108729. [CrossRef]
88. Bhuiyan, S.A.; Jameel, Y.; Chartrand, M.M.G.; St-Jean, G.; Gibson, J.; Bataille, C.P. Spatial variations in tap water isotopes across Canada: Tracing water from precipitation to distribution and assess regional water resources. *PLoS Water* **2023**, *2*, e0000068. [CrossRef]